

# Free energy of the Lennard-Jones solid

Martin A. van der Hoef

*Department of Chemical Engineering, University of Twente, P.O. Box 217, 7500 AE Enschede, The Netherlands*

(Received 12 April 2000; accepted 10 August 2000)

We have determined a simple expression for the absolute Helmholtz free energy of the fcc Lennard-Jones solid from molecular dynamics simulations. The pressure and energy data from these simulations have been fitted to a simple functional form (18 parameters) for densities ranging from around 0.94–1.20, and temperatures ranging from 0.1 to 2.0 (values in reduced Lennard-Jones units). The absolute free energy at an arbitrary state point in this range is obtained by integrating over density and temperature from the triple-point. Our result for the free energy is in very good agreement with the values reported in literature previously. Also the melting line obtained from our free energy expression, in combination with an equation of state for the liquid phase, is in excellent agreement with results by Agrawal and Kofke [Mol. Phys. **85**, 43 (1995)] obtained via the Gibbs–Duhem integration method. © 2000 American Institute of Physics. [S0021-9606(00)50342-0]

## I. INTRODUCTION

The Lennard-Jones (LJ) 6-12 potential is one of the most widely studied model potentials for simple fluids, owing to its simple functional form which greatly facilitates both theoretical evaluations and computer simulations, and yet proves to capture much of the essential physics. Although the potential is clearly an oversimplification—in particular it neglects higher-order dispersion interactions such as  $r^{-8}$  and  $r^{-10}$  attractions and three-body interactions—it gives surprisingly good results for the liquid properties of systems of closed-shell atoms or molecules, in particular of those which contain a high degree of spherical symmetry such as methane. But also for nonspherical molecules such as nitrogen, carbon dioxide, and even alkanes, the LJ potential may prove accurate if a temperature-dependent well-depth parameter  $\epsilon(T)$  is used.<sup>1–3</sup> Therefore, the determination of the thermodynamic properties of the ‘Lennard-Jonesium’ has been the subject of intense research over the past 40 years. The most fundamental (and most difficult to obtain) thermodynamic property of any system is the free energy. Once the Helmholtz free energy is known as function of density and temperature, any other thermodynamic quantity can be calculated. Moreover, the stability of a system with respect to some other system is directly related to the value of the free energy. There have been several attempts to determine an explicit functional form for the Helmholtz free energy of the LJ system for the liquid phase; one of the most accurate expressions has been obtained by Johnson *et al.*<sup>4</sup> (hereafter called the Johnson EoS), who have fitted a modified Benedict–Webb–Rubin-type expression to the data of a large number of molecular dynamics simulations. For a comparison of the Johnson EoS with other equations of state which have appeared in literature we refer to a recent paper by Mulero *et al.*<sup>5</sup> For the solid phase, the situation is different. Although over the years there have been many studies on the determination of the free energy of the LJ solid,<sup>6–10</sup> to our knowledge there does not exist a simple single expres-

sion for the free energy, analogous to the Johnson EoS for the liquid, at least not for densities and temperatures close the solid–liquid coexistence line. Broughton and Gilmer<sup>11</sup> have determined an expression for the free energy by thermodynamic integration of the internal energy from the harmonic crystal, but only for the  $P=0$  isochore. Lacks and Shukla<sup>12</sup> have obtained an expression for the anharmonic free energy from molecular dynamics simulation and perturbation theory in the density range  $\rho=0.864$  to  $\rho=1.0$ , and temperature range  $T=0$  to  $T=0.5$ , which is well below the triple-point, and therefore not applicable to solid–liquid coexistence properties. Moreover, the normal-mode frequencies required for the harmonic part of the free energy are not explicitly given, and have to be calculated separately to obtain the total free energy.

The goal of the present work is to obtain a simple but accurate expression for the Helmholtz free energy of the LJ solid (fcc) phase, in the same spirit as the Johnson EoS for the liquid phase. To this end, we have performed molecular dynamics simulations for a large number of state points (877 in total) for densities ranging from  $\rho=0.94$  to  $\rho=1.20$ , and temperatures ranging from  $T=0.1$  up to  $T=2.0$ . The data for the energy and pressure from the simulations have been fitted to polynomial functions of density and temperature. It should be noted that these fits cannot be determined independently, since the expression for energy and pressure should obey the Maxwell relation given by Eq. (6), which we will use explicitly in the derivation of the free energy. The absolute free energy at some arbitrary state-point can then be obtained by integrating the expressions for energy and pressure from some reference state-point, for which the free energy is known. For the liquid phase, one normally integrates from the ideal gas state, for which the absolute value of the free energy is known. However, this cannot be done for the solid phase, since along this path the system undergoes a phase transition. For our reference state point we have therefore chosen the triple-point, for which the absolute free energy can be obtained from an equation of state (EoS) for the liq-

uid, if the coexisting pressure is known. Thus both the triple-point temperature and an equation of state for the liquid are a prerequisite in our approach. This paper is organized as follows. In Sec. II we introduce an expression for the free energy from basic thermodynamic concepts. In Sec. III we discuss the details of the simulations and compare the results for the free energy with those from literature. In Sec. IV we calculate the melting line from the present EoS for the solid, in combination with the Johnson EoS for the liquid, and we have some concluding remarks in Sec. V.

## II. EXPRESSION FOR THE FREE-ENERGY

We consider a fcc crystal at finite temperature, where the particles interact via a Lennard-Jones potential,

$$\phi(r) = 4\epsilon \left( \left( \frac{\sigma}{r} \right)^{12} - \left( \frac{\sigma}{r} \right)^6 \right).$$

As is common for Lennard-Jones systems, we will use reduced units throughout the remainder of the paper, i.e., we define distances in units of  $\sigma$  and energies in units of  $\epsilon$ , from which follows that densities are in units of  $\sigma^{-3}$ , pressures in units of  $\epsilon\sigma^{-3}$ , and temperatures in units of  $\epsilon/k$ , where  $k$  is Boltzmann's constant.

We define the excess free energy per particle  $a^{\text{ex}}$  of the system at density  $\rho$  and inverse temperature  $\beta = 1/T$  as the total free energy  $a$  minus the free energy  $a^{\text{id}}$  of an ideal gas at the same density and inverse temperature, viz.,

$$\begin{aligned} a(\rho, \beta) &= a^{\text{id}}(\rho, \beta) + a^{\text{ex}}(\rho, \beta), \\ \beta a^{\text{id}}(\rho, \beta) &= \ln(\Lambda^3/e) + \ln \rho, \end{aligned} \quad (1)$$

where  $\Lambda$  is the de Broglie wavelength. In the same way we define the excess energy and pressure,

$$\begin{aligned} u(\rho, \beta) &= u^{\text{id}}(\rho, \beta) + u^{\text{ex}}(\rho, \beta), \quad u^{\text{id}}(\rho, \beta) = \frac{3}{2}\beta^{-1}, \quad (2) \\ \Pi(\rho, \beta) &= \Pi^{\text{id}}(\rho, \beta) + \Pi^{\text{ex}}(\rho, \beta), \quad \Pi^{\text{id}}(\rho, \beta) = (\rho\beta)^{-1}, \quad (3) \end{aligned}$$

where we have introduced  $\Pi = P/\rho^2$ , with  $P$  the pressure. The excess pressure and energy are related to the excess free energy via

$$\left( \frac{\partial \beta a^{\text{ex}}}{\partial \beta} \right)_\rho = u^{\text{ex}}(\rho, \beta), \quad \left( \frac{\partial a^{\text{ex}}}{\partial \rho} \right)_\beta = \Pi^{\text{ex}}(\rho, \beta). \quad (4)$$

Thus one can obtain the excess free energy for an arbitrary state-point  $(\rho, \beta)$  by integrating  $u^{\text{ex}}$  and  $\Pi^{\text{ex}}$  from a reference state-point  $(\rho_0, \beta_0)$ ,

$$\begin{aligned} \beta a^{\text{ex}}(\rho, \beta) - \beta_0 a^{\text{ex}}(\rho_0, \beta_0) &= \int_{\beta_0}^{\beta} u^{\text{ex}}(\rho, \beta') d\beta' \\ &+ \beta_0 \int_{\rho_0}^{\rho} \Pi^{\text{ex}}(\rho', \beta_0) d\rho'. \end{aligned} \quad (5)$$

The functions  $u^{\text{ex}}(\rho, \beta)$  and  $\Pi^{\text{ex}}(\rho, \beta)$  are not independent, however, since they should obey the Maxwell relation which follows from Eq. (4),

$$\left( \frac{\partial u^{\text{ex}}}{\partial \rho} \right)_\beta = \left( \frac{\partial \beta \Pi^{\text{ex}}}{\partial \beta} \right)_\rho, \quad (6)$$

from which follows that

$$\beta \Pi^{\text{ex}}(\rho, \beta) = b(\rho) + \frac{\partial U^{\text{ex}}(\rho, \beta)}{\partial \rho}, \quad (7)$$

where  $U^{\text{ex}}(\rho, \beta)$  is defined as the primitive function of  $u^{\text{ex}}(\rho, \beta)$ , with respect to  $\beta$ , and the "integration constant"  $b(\rho)$  is a yet unknown function of the density only. Inserting this into Eq. (5) gives

$$\begin{aligned} \beta a^{\text{ex}}(\rho, \beta) - \beta_0 a^{\text{ex}}(\rho_0, \beta_0) &= U^{\text{ex}}(\rho, \beta) - U^{\text{ex}}(\rho_0, \beta_0) \\ &+ \int_{\rho_0}^{\rho} b(\rho') d\rho'. \end{aligned} \quad (8)$$

For a crystal it is convenient to split the total excess energy into a harmonic (harm) and anharmonic (ah) part,

$$u^{\text{ex}}(\rho, \beta) = u^{\text{harm}}(\rho, \beta) + u^{\text{ah}}(\rho, \beta), \quad (9)$$

where the harmonic energy is equal to

$$u^{\text{harm}}(\rho, \beta) = u^{\text{stat}}(\rho) + \frac{3}{2}\beta^{-1}, \quad (10)$$

where the static energy  $u^{\text{stat}}$  is the excess energy at zero temperature, i.e., the energy of the atoms if positioned exactly at the fcc lattice sites. From a simple scaling argument it follows that for the Lennard-Jones potential,

$$u^{\text{stat}}(\rho) = c_2 \rho^2 + c_4 \rho^4. \quad (11)$$

The coefficients  $c_2$  and  $c_4$  have been evaluated numerically for the fcc lattice, and are found to be equal to

$$c_2 = -14.453\,920\,93, \quad c_4 = 6.065\,940\,096.$$

We next make the assumption that the anharmonic part of the excess energy  $u^{\text{ah}}(\rho, \beta)$  can be represented by the following functional form,

$$u^{\text{ah}}(\rho, \beta) = \sum_{n=0}^2 \sum_{m=2}^5 a_{nm} \rho^n \beta^{-m} \quad (12)$$

which form ensures that in the limit of low temperature the total excess energy approaches that of a harmonic crystal. From Eq. (7) then follows that

$$b(\rho) = \beta \Pi^{\text{ex}}(\rho, \beta) - \beta \frac{\partial u^{\text{stat}}(\rho)}{\partial \rho} - \frac{\partial U^{\text{ah}}(\rho, \beta)}{\partial \rho} \quad (13)$$

with

$$U^{\text{ah}}(\rho, \beta) = - \sum_{n=0}^2 \sum_{m=2}^5 a_{nm} \frac{1}{m-1} \rho^n \beta^{-m+1}. \quad (14)$$

We make the second assumption that the function  $b(\rho)$  can be represented by a polynomial in  $\rho$ ,

$$b(\rho) = \sum_{n=0}^3 b_n \rho^n.$$

From the above formulas we may finally write Eq. (8) as

$$\beta a^{\text{ex}}(\rho, \beta) = C(\rho_0, \beta_0) + \beta u^{\text{stat}}(\rho) + \frac{3}{2} \ln \beta + U^{\text{ah}}(\rho, \beta) + \sum_{n=0}^3 \frac{b_n}{n+1} \rho^{n+1}, \quad (15)$$

with

$$C(\rho_0, \beta_0) = \beta_0 a^{\text{ex}}(\rho_0, \beta_0) - \beta_0 u^{\text{stat}}(\rho_0) - \frac{3}{2} \ln \beta_0 - U^{\text{ah}}(\rho_0, \beta_0) - \sum_{n=0}^3 \frac{b_n}{n+1} \rho_0^{n+1}. \quad (16)$$

The absolute free energy is now completely determined by 18 parameters  $a_{nm}$  ( $n=0-2, m=2-5$ ),  $b_n$  ( $n=0-3$ ),  $c_2, c_4$ , and the absolute free energy of the reference point  $(\rho_0, \beta_0)$ ; the latter can be estimated from a single known point on the liquid–solid coexistence line. From the coexistence pressure  $P_{\text{coex}}$  at temperature  $\beta_0$  one can obtain the corresponding crystal density  $\rho_0$  from the EoS given above; the liquid density at coexistence  $\rho_l$  can be obtained from a separate EoS for the liquid, such as Johnson EoS. From the conditions for coexistence follows that

$$a^{\text{ex}}(\rho_0, \beta_0) = \beta_0^{-1} \ln(\rho_l / \rho_0) + a_{\text{liq}}^{\text{ex}}(\rho_l, \beta_0) + P_{\text{coex}} \frac{\rho_0 - \rho_l}{\rho_0 \rho_l}, \quad (17)$$

where the absolute free energy  $a_{\text{liq}}^{\text{ex}}$  can be obtained from the liquid EoS. The values for the parameters which determine the equation of state described above will be obtained by fitting the expressions for energy and pressure to the data from molecular dynamics simulations for a large number of state-points, which is described in the next section.

### III. RESULTS FROM MOLECULAR DYNAMICS SIMULATION

From molecular dynamics simulation we have evaluated  $u^{\text{ex}}(\rho, \beta)$  and  $\Pi^{\text{ex}}(\rho, \beta)$  for a total of 877 different state-points  $(\rho, \beta)$ , in the density range from around  $\rho=0.94$  to  $\rho=1.2$ , but not smaller than the melting density, and for temperatures ranging from  $T=0.1$  to  $T=2.0$ . The system contained 2048 particles, and periodic boundary conditions were employed. The particles were interacting via a Lennard-Jones potential which was truncated (but not shifted) at a distance  $r_c=6$ , which was in any case smaller than half the periodic box-length. We have added the usual long-range correction to the values for energy and pressure obtained with the truncated potential,

$$u^{\text{ex}}(\rho, \beta) = u_{\text{trunc}}^{\text{ex}}(\rho, \beta) - \frac{8}{3} \pi r_c^{-3} \rho,$$

$$\Pi^{\text{ex}}(\rho, \beta) = \Pi_{\text{trunc}}^{\text{ex}}(\rho, \beta) - \frac{16}{3} \pi r_c^{-3}.$$

Note that in these corrections it is assumed that the radial distribution function equals one from the cut-off value to infinity; This might be a valid approximation for the liquid phase, however for the crystal phase this is not true, as shown in Fig. 1, where we show the  $g(r)$  for a much larger system (8000 particles) at density  $\rho=1.2$  and  $T=1.0$ . However, the error that is made in the correction term by assuming that  $g(r)=1$  beyond  $r=6$  is small, where it should be

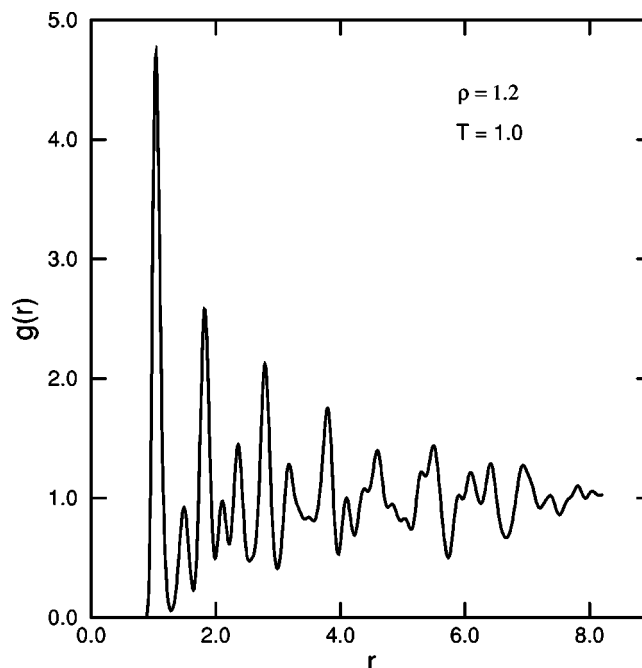


FIG. 1. Radial distribution function of the fcc Lennard-Jones system at a density  $\rho=1.2$  and temperature  $T=1.0$ .

noted that the correction term itself is relatively small (except for very low temperatures), since we have used a rather large cut-off value. The systems were equilibrated for 1000 time steps from their initial state in which the particles were positioned at the fcc lattice sites with a Maxwellian velocity distribution. Production runs during which pressure and energy were recorded lasted 50 000 time steps, where the temperature was kept at a constant value via a Nosé–Hoover

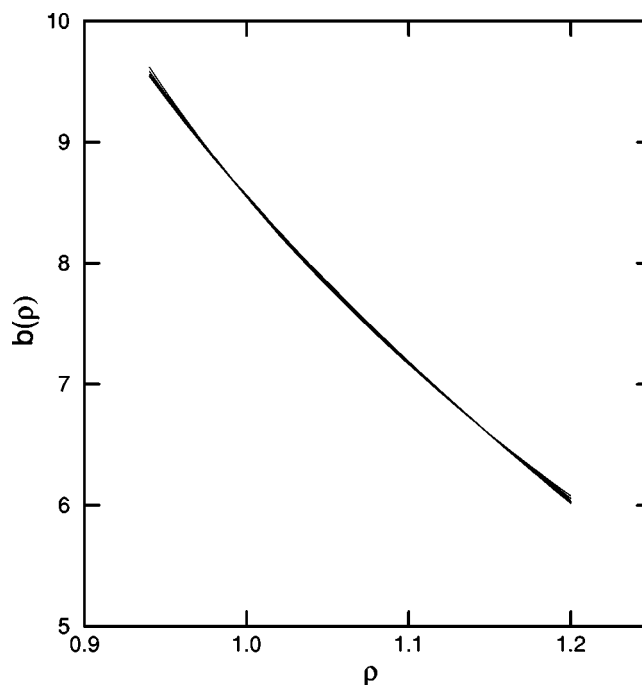


FIG. 2.  $b(\rho)$  constructed according to Eq. (13) from the simulation data for the pressure and the fit parameters  $a_{nm}$ , for various inverse temperatures  $\beta$ . The results for different  $\beta$  are almost indistinguishable.

TABLE I. Values for the parameters in Eqs. (19)–(21).

| n | $a_{n2}$    | $a_{n3}$    | $a_{n4}$    | $a_{n5}$    | $b_n$       |
|---|-------------|-------------|-------------|-------------|-------------|
| 0 | -8.215 1768 | 12.070 686  | -6.659 4615 | 1.321 1582  | 69.833 875  |
| 1 | 13.404 069  | -20.632 066 | 11.564 825  | -2.306 4801 | -132.869 63 |
| 2 | -5.548 1261 | 8.846 5978  | -5.025 8631 | 1.007 0066  | 97.438 593  |
| 3 | ...         | ...         | ...         | ...         | -25.848 057 |

thermostat. The parameters  $a_{nm}$  in Eq. (12) were obtained by a least-square fit to the simulation data for the anharmonic energy, where we used the singular value decomposition method.<sup>13</sup> We should note that in this fit we have given less weight to the data for temperatures lower than 0.3; we will come back to this point in the discussion in Sec. V. From the resulting fit parameters  $a_{nm}$  and the simulation data for  $\Pi^{\text{ex}}(\rho, \beta)$ , the function  $b(\rho)$  can be constructed according to Eq. (13). Note that both the functions  $U^{\text{ah}}(\rho, \beta)$  and  $\Pi^{\text{ex}}(\rho, \beta)$  depend on  $\beta$ , however  $b(\rho)$  itself should *not* depend on  $\beta$ . This is indeed the case, as shown in Fig. 2, where we have plotted  $b(\rho)$  as function of  $\rho$  for all 35 values of  $\beta$  studied in the range  $T=0.3$  to  $T=2.0$ . The data for different  $\beta$  all fall onto a single curve, which indicates that the simulation data are thermodynamically consistent, i.e., the data for pressure and energy obey the Maxwell relation (6). The curve shown in Fig. 2 has been fitted to a polynomial of order 3 to obtain the parameters  $b_n$ . The final values obtained for both  $a_{nm}$  and  $b_n$  from the procedure described above are given in Table I. In order to obtain the absolute free energy, we choose the triple-point as our reference state point. From a triple-point temperature  $T_{\text{tr}}$  we can determine the triple point pressure by implying the conditions for coexistence (equal pressure and equal chemical potential) for the gas and the liquid phase at that temperature. The values for the gas phase are calculated from the virial equation of state up to the third virial coefficient, and the values for the liquid phase are calculated from the Johnson EoS. Once the coexisting pressure is determined, we evaluate the excess free energy of the solid at the triple-point from Eq. (17), from which the constant  $C$  can be determined according to Eq. (16). We have performed this procedure for various values of the triple point temperature ranging from 0.683 to 0.691. The coefficient  $C$  was found to fit well to the following function of the triple-point temperature,

$$C(T_{\text{tr}}) = -19.450\,3982 - 8.891\,038\,55 \cdot T_{\text{tr}} + 4.689\,854\,18 \cdot T_{\text{tr}}^2 \quad (18)$$

From the equations of Sec. II, we thus finally arrive at the following expressions for energy, pressure and Helmholtz free energy of the solid fcc state,

$$u^{\text{ex}}(\rho, \beta) = u^{\text{stat}}(\rho) + \frac{3}{2}\beta^{-1} + u^{\text{ah}}(\rho, \beta), \quad (19)$$

$$\frac{\beta P^{\text{ex}}}{\rho^2} = \beta \frac{\partial u^{\text{stat}}(\rho)}{\partial \rho} + \frac{\partial U^{\text{ah}}(\rho, \beta)}{\partial \rho} + \sum_{n=0}^3 b_n \rho^n, \quad (20)$$

$$\beta a^{\text{ex}}(\rho, \beta) = C(T_{\text{tr}}) + \beta u^{\text{stat}}(\rho) + \frac{3}{2} \ln \beta + U^{\text{ah}}(\rho, \beta) + \sum_{n=0}^3 \frac{b_n}{n+1} \rho^{n+1}, \quad (21)$$

where  $u^{\text{stat}}(\rho)$ ,  $u^{\text{ah}}(\rho, \beta)$ ,  $U^{\text{ah}}(\rho, \beta)$ , and  $C(T_{\text{tr}})$  are given by Eqs. (11), (12), (14), and (18), respectively. For the triple-point temperature we choose the value  $T_{\text{tr}}=0.687$  from Agrawal and Kofke.<sup>1</sup> From Eq. (18) then follows that

$$C = -23.345\,0759, \quad (22)$$

which value we will use in the remainder of the paper.

As a first test of the validity of expression (21) we investigate the limit of low temperature, in which case the free energy should approach that of a harmonic crystal, which can be calculated from a normal-mode analysis. In the limit of  $T$  small, Eq. (21) reduces to

$$\lim_{\beta \rightarrow \infty} \beta a^{\text{ex}}(\rho, \beta) = -23.345\,0759 + \beta u^{\text{stat}}(\rho) + \frac{3}{2} \ln \beta + \sum_{n=0}^3 \frac{b_n}{n+1} \rho^{n+1},$$

which is equal to the free energy of a harmonic crystal if

$$\frac{1}{N} \sum_{i=1}^{3N-3} \ln \omega_i(\rho) = -23.345\,0759 + \sum_{n=0}^3 \frac{b_n}{n+1} \rho^{n+1} + \ln \rho + \frac{3}{2} \ln(2\pi) - 1, \quad (23)$$

where  $\omega_i$  are the normal-mode frequencies. In Table II we compare the LHS of Eq. (23) with the RHS for five different densities, where the normal-mode frequencies are taken from Lacks and Rutledge,<sup>14</sup> Table I. We find that the agreement is within 0.5%. After having confirmed that the expression (21) has the correct low-temperature behavior, we next compare in Fig. 3 with results from literature at finite temperatures. In Fig. 3 the lines represent the free energy calculated from Eq. (21) at temperatures 0.75, 1.15, and 1.35; the open symbols are the results obtained by Monte Carlo simulation,<sup>7</sup> the

TABLE II. Comparison of the low-temperature limit of the free energy expression with the normal-mode frequencies.

| $\rho$ | $\frac{1}{N} \sum_i \ln \omega_i(\rho)$ | RHS of Eq. (23) |
|--------|-----------------------------------------|-----------------|
| 0.9423 | 7.210                                   | 7.248           |
| 0.9706 | 7.503                                   | 7.540           |
| 1.0000 | 7.790                                   | 7.828           |
| 1.0306 | 8.070                                   | 8.113           |
| 1.0625 | 8.346                                   | 8.395           |

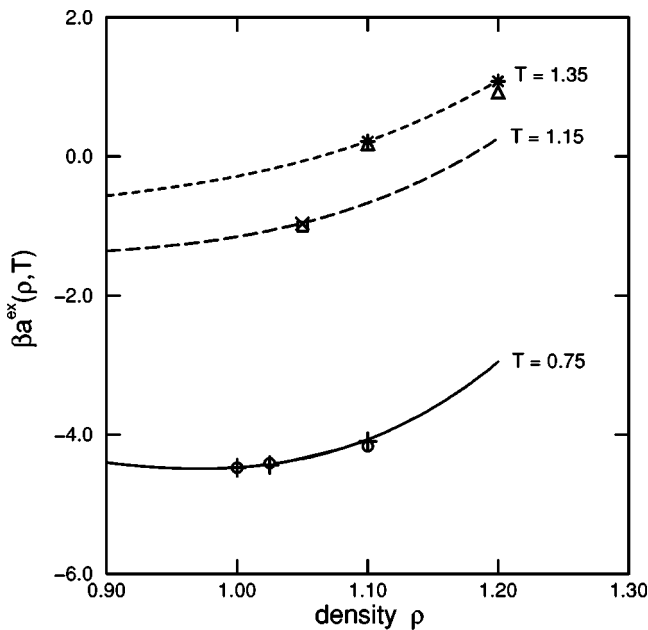


FIG. 3. Excess free energy divided by temperature as a function of density at three different temperatures. The lines follow from the expression derived in this paper. The open circles, squares and triangles are from Monte Carlo simulations at temperatures  $T=0.75$ ,  $T=1.15$ , and  $T=1.35$ , respectively (Ref. 7). The plus-, cross-, and star-symbols are from perturbation theory at temperatures  $T=0.75$ ,  $T=1.15$ , and  $T=1.35$ , respectively (Ref. 7).

plus-, cross-, and star-symbols are calculated from perturbation theory.<sup>7</sup> Again the agreement is good to very good.

#### IV. APPLICATION TO THE MELTING LINE

From the expression for the free energy of the solid obtained in the previous section, combined with the expression for free energy of the liquid from the Johnson EoS, we have calculated the liquid–solid coexistence line by equating the chemical potential and pressure for both phases. In Fig. 4 we compare our results (solid lines) with the results from Agrawal and Kofke (open symbols) which were obtained by the Gibbs–Duhem integration method.<sup>1</sup> We find excellent agreement between the two results; it should be borne in

mind however that the location of “our” triple-point is equal to that of Agrawal and Kofke by construction. It was suggested by these authors that the coexistence pressure can be well represented by the following function:

$$P_{\text{coex}} = \beta^{-5/4} \exp(-0.4759 \beta^{1/2}) [16.89 + A\beta + B\beta^2], \quad (24)$$

which satisfies the soft-sphere result for  $\beta \rightarrow 0$ . We find that this expression fits the coexistence pressure extremely well, where inclusion of higher powers of  $\beta$  in Eq. (24) will not give any improvement. From our data we obtain the values  $A = -7.2866$  and  $B = -2.9895$ , where Agrawal and Kofke found the values  $A = -7.19$  and  $B = -3.028$ . For completeness we also give expressions for the liquid density  $\rho_{\text{liq}}$  and the solid density  $\rho_{\text{sol}}$  at coexistence, which are found to be well described by the following fits:

$$\rho_{\text{liq}} = \beta^{-1/4} [0.91070 - 0.25124\beta + 0.85861\beta^2 - 1.08918\beta^3 + 0.63932\beta^4 - 0.14433\beta^5], \quad (25)$$

$$\rho_{\text{sol}} = \beta^{-1/4} [0.92302 - 0.09218\beta + 0.62381\beta^2 - 0.82672\beta^3 + 0.49124\beta^4 - 0.10847\beta^5]. \quad (26)$$

Next, we compare the melting line with the experimental results for argon<sup>15</sup> and krypton,<sup>16</sup> see Fig. 5. The experimental data has been reduced by the Lennard-Jones parameters  $\epsilon/k = 119.8$  K and  $\sigma = 0.3405$  nm for argon, and  $\epsilon/k = 172.7$  K and  $\sigma = 0.3591$  nm for krypton, which are obtained from a fit of the second virial coefficient to experimental PV-data.<sup>17</sup> We find that the Lennard-Jones potential with these parameters describe the solid–liquid coexistence properties very well, which is to some extent remarkable since the LJ parameters have been obtained from gas-phase data. We also compare with results<sup>18</sup> obtained by perturbation theory for the two-body Aziz potential plus an approximation to the Axilrod–Teller triple-dipole three-body potential (open symbols in Fig. 6). It is shown that the Lennard-Jones potential gives a better agreement with experiment than the full three-body potential. One cause might be the approximate nature of the three-body interactions in Ref. 18; in that paper they use an effective isotropic  $r^{-9}$  potential,

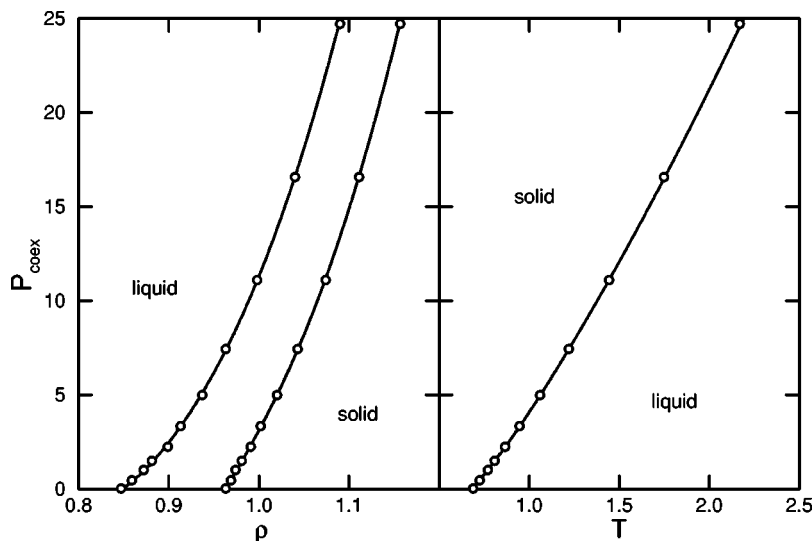


FIG. 4. Coexistence pressure vs density (left) and vs temperature (right) for the fcc-liquid Lennard-Jones system. The solid lines follow from the expression for the free energy derived in this paper. The open symbols are the results by Agrawal and Kofke (Ref. 1).

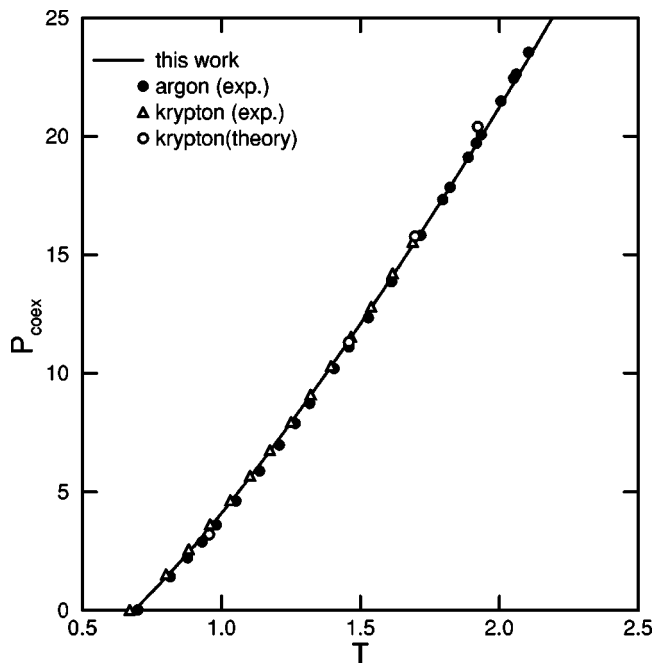


FIG. 5. Coexistence pressure vs temperature for the fcc-liquid Lennard-Jones system. The solid line is the same as in Fig. 4. The filled circles and open triangles are the experimental results for argon and krypton, respectively. The open circles are the results from perturbation theory for krypton, where the atoms interact via a two-body Aziz potential plus a three-body Axilrod–Teller potential. The data for argon and krypton have been reduced by the Lennard-Jones parameters derived from gas-phase data.

instead of the full an-isotropic three-body potential. A second cause might be the neglect of higher-order dispersion interactions in the three-body potential. Recently,<sup>19</sup> it was found that the dipole–dipole–quadrupole three-body forces contribute substantially to the pressure in dense liquids, bringing the results from simulation very close to the experimental results for argon.

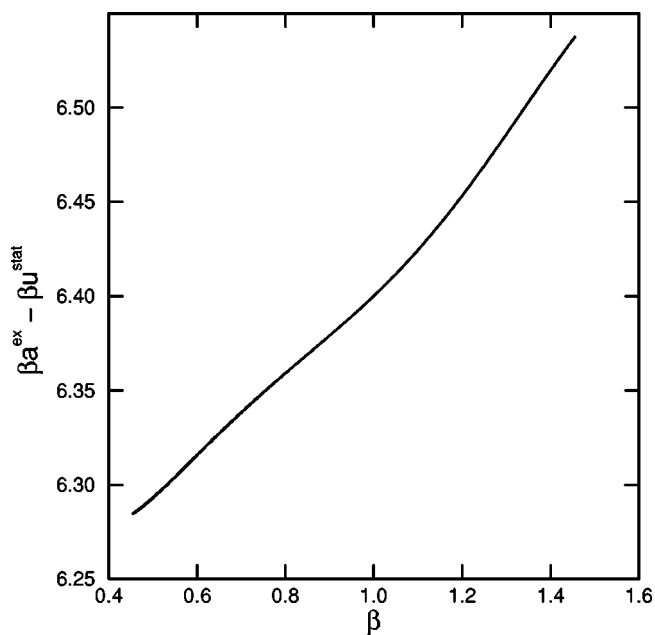


FIG. 6. The “Ross constant”  $\beta a^{\text{ex}} - \beta u^{\text{stat}}$  along the melting line, as function of  $\beta$ .

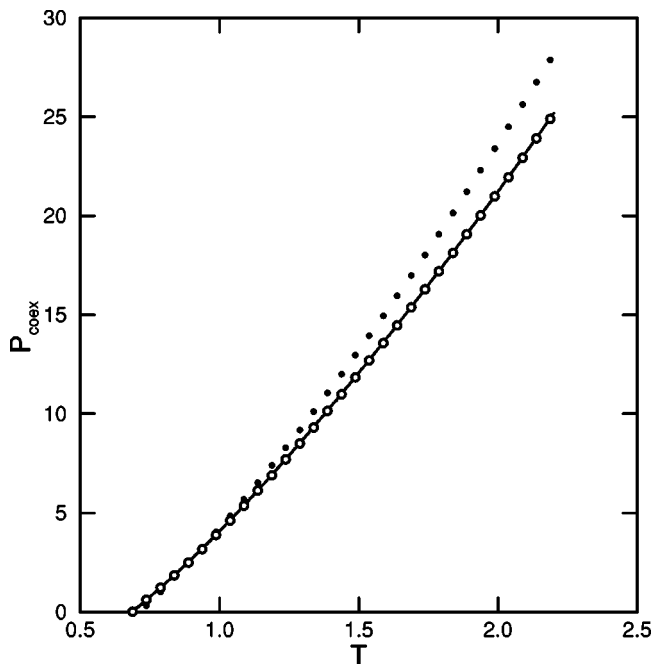


FIG. 7. Coexistence pressure calculated from Ross' melting rule (solid symbols), compared with the true coexistence pressure (solid line) and the coexistence pressure calculated from Eq. (29) (open symbols).

Finally, we test the validity of Ross' melting rule,<sup>20</sup> which states that along the melting line,

$$\beta a^{\text{ex}} - \beta u^{\text{stat}} = \text{constant}, \tag{27}$$

which follows from the assumption that along the melting line the reduced free volume of the crystal is constant. For the inverse power potential  $r^{-n}$  the relation is exact, where the constant is around 6 for all values of  $n$ .<sup>21</sup> From the present expression for the free energy (21) we can write Eq. (27) as

$$\frac{3}{2} \ln \beta + U^{\text{ah}}(\rho, \beta) + \sum_{n=0}^3 \frac{b_n}{n+1} \rho^{n+1} = \text{constant}. \tag{28}$$

In Fig. 6 we show  $\beta a^{\text{ex}} - \beta u^{\text{stat}}$  as a function of inverse temperature along the melting line. We find the same result as Agrawal and Kofke,<sup>1</sup> namely, a slight variation in Ross' “constant” from 6.30 to 6.55. Although this variation might seem relatively small, it is still too large for the coexistence pressure to be accurately predicted from Ross' rule. In Fig. 7 the filled symbols indicate the coexistence pressure obtained by solving Eq. (28) for one particular value of the constant (at  $\beta=1.1$ ). We find rather large deviations from the true coexistence pressure, given by the solid line (same as in Fig. 4). The functional form of Ross' constant shown in Fig. 6 suggests that we could accurately predict the melting line from the following “empirical” modification to the Ross melting rule

$$\beta a^{\text{ex}} - \beta u^{\text{stat}} = \begin{cases} 6.034 + 0.348\beta & \beta < 1.1, \\ 6.191 + 0.205\beta & \beta \geq 1.1. \end{cases} \tag{29}$$

The coexistence pressure obtained by solving Eq. (29) (Fig. 7, open symbols) is found to be in very close agreement with the true coexistence pressure.

## V. DISCUSSION

We would like to conclude with a few remarks.

First, we note that in the fit procedure as described in Sec. III we have also included data for temperatures lower than 0.3, since we want to explore the low-temperature limit of our function in order to compare with the normal-mode frequencies. It turned out however that the functions could not fit the low-temperature data with as high accuracy as for temperatures equal or higher than 0.3, since for lower temperatures the finite size effects become relatively large, and the inadequacy of the ‘‘standard’’ correction (e.g.  $8\pi r_c^{-3}\rho/3$ ) becomes noticeable. In particular, the functions  $b(\rho)$  constructed at temperatures smaller than 0.3 did slightly deviate from the curve as shown in Fig. 2, which indicates that there is some inconsistency with respect to the pressure and energy data, which could be well caused by finite size effects. We have therefore given the low-temperature data less weight in the fitting procedure than the high-temperature data, so that the function (21) is expected to be most accurate in the temperature range  $T=0.3$  to  $T=2.0$ , and less accurate (but still valid), for lower temperatures. This could be the cause of the (very small) deviation with the normal-mode frequencies as shown in Table II.

Second, our expression for the *absolute* free energy depends directly on the reported value for the triple-point temperature. Any new and improved estimate of this temperature could be readily used in the present EoS, since it would only change the ‘‘offset’’ value  $C$  [see Eq. (18)], and *not* the values for the parameters  $a_{nm}$  and  $b_n$ . Because of this dependence on the triple-point value, we have not attempted to put strict confidence limits on the final result for the free energy, which would in any case be a nontrivial task; the error in the final expression for the free energy not only depends on the error in the simulation data, but also on the error in the Johnson EoS (which is not known); these errors also have an indirect impact via the estimates for the coexisting densities at the triple-point, which are used in both the liquid and solid EoS to obtain the offset value in the total free energy. This procedure makes it very difficult to put reliable confidence limits on the final result, where the largest error is expected to follow in any case from the estimate of the triple-point temperature.

Third, we would like to stress that the particular form of the functions to which energy and pressure have been fitted has not been guided by considerations from statistical mechanics, other than splitting the quantities into harmonic and anharmonic parts, and imposing the Maxwell relation for en-

ergy and pressure. Rather, we have chosen simple polynomial functions to which the data could be fitted with good accuracy. The purpose of this work is therefore not to give any new insight from a statistical mechanics point of view, but to provide with an expression for *practical* purposes, i.e., from which any thermodynamic quantity of the solid can be easily obtained with good accuracy, which can be used instead of a molecular dynamics or Monte Carlo simulation to verify results from theory. Moreover, quantities that are difficult to obtain from simulation with good accuracy (such as the compressibility or the heat capacity) can be obtained straightforwardly from the present equation of state. Another application could be found in studies of systems with more complicated potentials (such as three-body, or two-center potentials) for which the Lennard-Jones potential could serve as a reference potential, and the thermodynamic properties from the potential of interest can be obtained by thermodynamic integration. Since the knowledge of the free energy of the reference system is a prerequisite in such an approach, the present equation of state could serve useful. Work along these lines to obtain the free energy for solid nitrogen is currently underway.

## ACKNOWLEDGMENTS

I would like to thank Wim Briels and Harald Tepper for useful and stimulating discussions.

- <sup>1</sup>R. Agrawal and D. A. Kofke, *Mol. Phys.* **85**, 43 (1995).
- <sup>2</sup>J. S. Rowlinson, *Trans. Faraday Soc.* **50**, 647 (1954); **51**, 1317 (1955).
- <sup>3</sup>T. Sun and A. S. Teja, *J. Phys. Chem.* **100**, 17365 (1996).
- <sup>4</sup>J. K. Johnson, J. A. Zollweg, and K. E. Gubbins, *Mol. Phys.* **78**, 591 (1993).
- <sup>5</sup>A. Mulero, C. A. Faúndez, and F. Cuadros, *Mol. Phys.* **97**, 453 (1999).
- <sup>6</sup>J. P. Hansen and E. F. Pollock, *J. Chem. Phys.* **62**, 4581 (1975).
- <sup>7</sup>H. S. Kang, T. Ree, and F. H. Ree, *J. Chem. Phys.* **84**, 4547 (1986).
- <sup>8</sup>J. M. Rickman and S. R. Phillpot, *J. Chem. Phys.* **95**, 7562 (1991).
- <sup>9</sup>Y. Choi, T. Ree, and F. H. Ree, *J. Chem. Phys.* **99**, 9917 (1993).
- <sup>10</sup>R. C. Shukla and E. R. Cowley, *Phys. Rev. B* **58**, 2596 (1998).
- <sup>11</sup>J. Q. Broughton and G. H. Gilmer, *J. Chem. Phys.* **79**, 5095 (1983).
- <sup>12</sup>D. J. Lacks and R. C. Shukla, *Phys. Rev. B* **54**, 3266 (1996).
- <sup>13</sup>W. H. Press, S. A. Teukolsky, W. T. Vetterling, and B. P. Flannery, *Numerical Recipes* (Cambridge University Press, Cambridge, 1992).
- <sup>14</sup>D. J. Lacks and G. C. Rutledge, *J. Chem. Phys.* **101**, 9961 (1994).
- <sup>15</sup>W. H. Hardy, R. K. Crawford, and W. B. Daniels, *J. Chem. Phys.* **54**, 1005 (1971).
- <sup>16</sup>R. K. Crawford and W. B. Daniels, *J. Chem. Phys.* **55**, 5651 (1971).
- <sup>17</sup>J. O. Hirschfelder, C. F. Curtiss, and R. B. Bird, *Molecular Theory of Gases and Liquids* (Wiley, New York, 1964).
- <sup>18</sup>J. H. Kim, T. Ree, and F. H. Ree, *J. Chem. Phys.* **91**, 3133 (1989).
- <sup>19</sup>M. A. van der Hoef and P. A. Madden, *J. Chem. Phys.* **111**, 1520 (1999).
- <sup>20</sup>M. Ross, *Phys. Rev.* **184**, 233 (1969).
- <sup>21</sup>W. G. Hoover, S. G. Gray, and K. W. Johnson, *J. Chem. Phys.* **55**, 1128 (1971).